Weierstraß-Institut
für Angewandte Analysis und Stochastik

On unwanted nucleation phenomena at the wall of a VGF chamber

Wolfgang Dreyer[1], Frank Duderstadt[1],

Stefan Eichler[2], Margarita Naldzhieva[1]

submitted: 25th March 2008

[1] Weierstrass Institute
for Applied Analysis and Stochastics
Mohrenstraße 39
D – 10117 Berlin
Germany
E-Mail: dreyer@wias-berlin.de
        dudersta@wias-berlin.de
        naldzhie@wias-berlin.de
	[2] Freiberger Compound Materials GmbH
	
	Am Junger Löwe Schacht 5
	D – 09599 Freiberg / Sachsen
	Germany
	E-Mail: eichler@fcm-germany.com

WIAS

Abstract

This is preliminary study on a phenomenon that happens during crystal growth of GaAs in a vertical gradient freeze (VGF) device. Here unwanted polycrystals nucleate at the chamber wall and move into the interior of the crystal. This happens within an undercooled region in the vicinity of the triple point, where the liquid-solid interface meets the chamber wall. The size and shape of that region is modelled by the Gibbs-Thomson law, which will be rederived in this paper. Hereafter we identify the crucial parameter, whose proper adjustment may minimize the undercooled region. Finally we give a simple estimate to calculate and evaluate the energy barrier for homogeneous and heterogeneous nucleation of a solid nucleus in the undercooled melt.

1   Introduction

This is the first of two studies on a phenomenon that happens during crystal growth of GaAs in a vertical gradient freeze (VGF) device. Here unwanted polycrystals nucleate at the chamber wall and move into the interior of the crystal. This happens within an undercooled region in the vicinity of the triple point, where the liquid-solid interface meets the chamber wall. In the current study we describe the phenomena ignoring the difference between the heat conductivities of solid and liquid, its influence will be addressed in a further study.
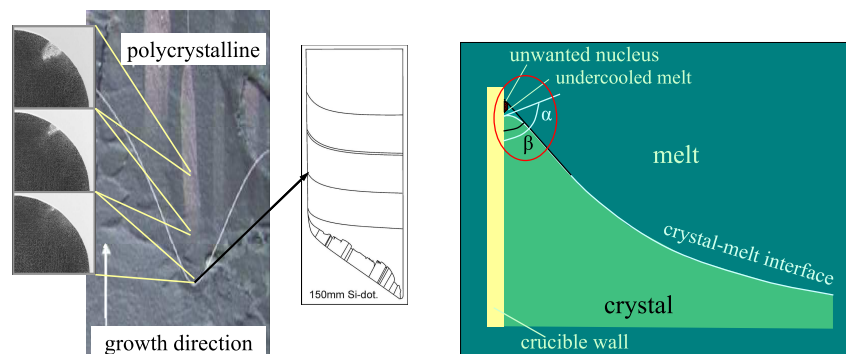

Figure 1: *Nucleation in the undercooled region in the melt*

The paper is organized as follows. In section 2 we give the necessary conditions for local equilibrium in a general solid-liquid system with sharp interface. From these we re-derive the Gibbs-Thomson law, which is the basis of the mathematical models presented in the next two sections.

In section 3 we introduce a general model for the temperature distribution and the crystal-melt interface in the vicinity of the triple point. In the case of equal liquid and solid thermal conductivity coefficients, we provide an exact solution of

1

the stationary heat equation and determine the interface as a simple smooth curve in an appropriate coordinate system. Hereafter we identify the parameter, whose proper adjustment may minimize the undercooled region.

In section 4 we give a simple estimate of the critical number of particles needed for the nucleation of a solid nucleus in the melt. We show the difference between the homogeneous and the heterogeneous case and calculate the critical number for typical parameter values.

Finally, in section 5 we briefly discuss the results from the previous two sections.

2 The liquid-solid system with sharp interface at local equilibrium

The main thermodynamical relation used in this paper is the Gibbs-Thomson law, which links the temperature of the liquid-solid interface to its mean curvature if the interface is in local equilibrium. The resulting formula we will apply to three different situations (see Figure 2) in the general frame of a liquid-solid system with sharp interface.
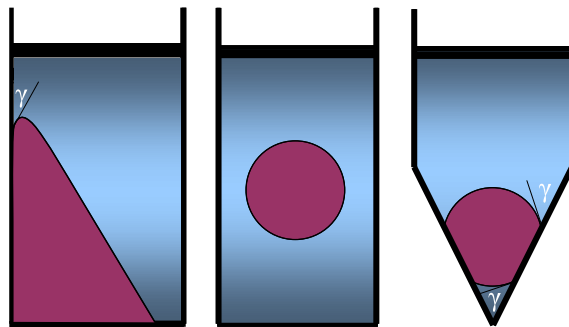

Figure 2: *Liquid-solid systems: Left: Crystal-melt interface in the vicinity of the triple point. Middle and Right: Homogeneous and heterogeneous nucleation*

In this section we consider a closed unitary solid-liquid system with curved interface. We introduce the following notation:

$T_{L/S}:$	temperature in liquid/solid
$q_{L/S}:$	heat flux in liquid/solid
$p_{L/S}:$	pressure in liquid/solid
$V_{L/S}:$	volume of liquid/solid
$m_{L/S}:$	mass of liquid/solid
$m:$	mean atomic mass of GaAs
$n:$	total number of atoms in the solid
$\rho_{L/S}:$	density of liquid/solid
$\sigma_{LW/SW}:$	surface tension of liquid-wall/solid-wall interface
σ or $\sigma_{SL}:$	surface tension of solid-liquid interface
$\kappa_M:$	mean curvature of solid-liquid interface
$\gamma:$	contact angle of wall and solid-liquid interface
$\psi:$	specific Helmholtz free energy
$s:$	specific entropy

2.1 Necessary conditions for equilibrium

We use three kinds of conditions to describe the properties of the solid-liquid interface.

Mechanical conditions:

(i) $p_S = p_L + 2\sigma_{SL}\kappa_M$, where the sign of the mean curvature κ_M must be chosen so that we find the higher pressure on the convex side of the interface.

(ii) $\cos(\gamma) = \dfrac{\sigma_{SW} - \sigma_{LW}}{\sigma_{SL}}$.

Thermal condition:

(iii) $T_S = T_L =: T_I$.

(iv) $q_S = q_L$.

Phase condition:

(v) $g_S(T_I, p_S) = g_L(T_I, p_L)$.

The mechanical condition (i) is the Young-Laplace law, which relates the pressure at the interface to its mean curvature. The meaning of the angle γ in condition (ii) is given in Figure 2), see [DK] for details. The thermal condition (iii) is part of the axioms that establish the 2$^{\text{nd}}$ law of thermodynamics, and (iv) describes the

continuity of the heat flux that we have at an interface at rest. The phase condition (v) states the continuity of the specific Gibbs energy if the interface is in local phase equilibrium, and it is also derived in [DK]. That continuity represents the basis of the Gibbs-Thomson law.

The specific Gibbs energy is defined by $g = \psi + \frac{p}{\rho}$ and fulfils the Gibbs equation

$$dg = -sdT + \frac{1}{\rho}dp. \tag{1}$$

2.2 Plane interface

In the case $\kappa_M \equiv 0$ the interface between the two phases is plane. Here not only the specific Gibbs energy, but also the pressure is continuous across the interface:

$$p_L = p_S := \bar{p} \quad \text{and} \quad g_L(T, \bar{p}) = g_S(T, \bar{p}). \tag{2}$$

The so called melting pressure $\bar{p}$ may be calculated from $(2)_2$ as a function of the temperature T. By means of some constitutive laws one can then compute the corresponding mass densities $\bar{\rho}_S$ and $\bar{\rho}_L$.

2.3 The Gibbs-Thomson law

In order to re-derive the Gibbs-Thomson law, we expand the specific Gibbs energy of liquid and solid in the vicinity of the point $(T_m, \bar{p}(T_m))$, where T_m is the melting temperature, which can be read off for given pressure $\bar{p}$ from a classical phase diagram for a plane interface. By means of the Gibbs equation (1) we obtain the approximation

$$\begin{aligned} g(T_I, p) &= g\left(T_m + (T_I - T_m), \bar{p} + (p - \bar{p})\right) \\ &\approx g(T_m, \bar{p}) - \bar{s}(T_I - T_m) + \frac{1}{\bar{\rho}}(p - \bar{p}), \end{aligned}$$

with $\bar{p} = \bar{p}(T_m), \bar{s} = \bar{s}(T_m)$ and $\bar{\rho} = \bar{\rho}(T_m)$ for liquid and solid, respectively. We may now use $(2)_2$ to compute the difference between the liquid and solid Gibbs energy

$$g_S(T_I, p_S) - g_L(T_I, p_L) = \lambda\left(\frac{T_I}{T_m} - 1\right) + \left(\frac{1}{\bar{\rho}_S} - \frac{1}{\bar{\rho}_L}\right)(p_L - \bar{p}) + \frac{1}{\bar{\rho}_S}2\sigma\kappa_M, \tag{3}$$

where $\lambda = (\bar{s}_L - \bar{s}_S)T_m$ is the melting heat, also called latent heat, which is positive for GaAs. At interfacial equilibrium, when the energy of liquid and solid is equal, equation (3) simplifies to

$$T_I = T_m\left(1 + \frac{1}{\lambda}\left(\frac{1}{\bar{\rho}_L} - \frac{1}{\bar{\rho}_S}\right)(p_L - \bar{p})\right) - \frac{T_m}{\lambda\bar{\rho}_S}2\sigma\kappa_M. \tag{4}$$

For the temperature $\bar{T}(p_L)$ in a plane interface system with liquid pressure p_L the last term in equation (4) vanishes, thus it holds

$$\bar{T}(p_L) = T_m \left(1 + \frac{1}{\lambda} \left(\frac{1}{\bar{\rho}_L} - \frac{1}{\bar{\rho}_S} \right) (p_L - \bar{p}) \right). \tag{5}$$

This is for example the temperature at the melting isotherm in Figure 3_1. For a curved interface we tus obtain

$$T_I = \bar{T}(p_L) - \frac{\sigma T_m}{\lambda \bar{\rho}_S} 2\kappa_M. \tag{6}$$

This equation is known as the Gibbs-Thomson law.

3 The interface model in the vicinity of the triple point

3.1 General model

In this section we study (i) the temperature distribution in the crystal-melt region between the melting isothermal line and the crucible wall, and (ii) the shape of the interface at equilibrium. For symmetry reasons, we confine our analysis to the problem in a plane and fix an appropriate coordinate system (see Figure 3_2), which choice makes further calculations easier. We assume that in this setting the interface I can be represented as the graph of a smooth function $y(x)$.
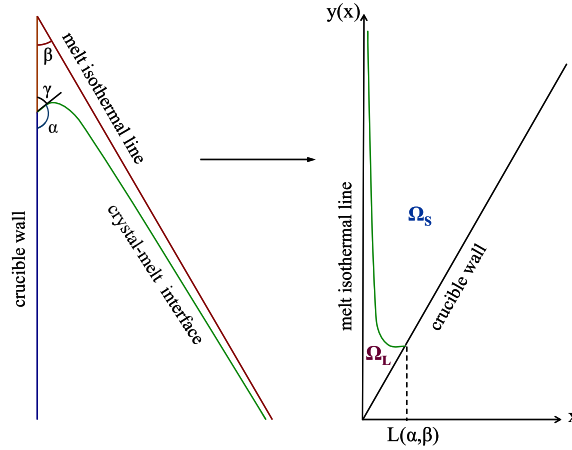

Figure 3: *General setting and appropriate transformation in 2D*

We denote by β the angle between the crucible wall and the melt isothermal and by γ the contact angle of the wall and the crystal-melt interface. Sometimes we use $\alpha = \pi - \gamma$ instead. Typical parameter values are $\alpha \in [90°, 130°]$,see [Hur], and $\beta \in [0.5°, 20°]$, see [EKSJ]. The coordinate of the triple point L is still to be determined.

Our goal is to identify the function $y(x)$ and the temperature T_I at the interface. For this purpose we have to solve the stationary heat equation (i.e. Laplace equation) in the liquid Ω_L and in the solid domain Ω_S, respectively, subjected to the interfacial conditions (iii) and (iv) from Section 2.1 and the Gibbs-Thomson law (6):

$$\Delta T_{L/S} = 0 \quad \text{in} \quad \Omega_{L/S} \qquad \text{with} \quad \begin{cases} T_L = T_S \equiv T_I \\ \\ a_L \, \nabla T_L \cdot \vec{n} = a_S \, \nabla T_S \cdot \vec{n} \end{cases} \quad \text{on} \quad I, \qquad (7)$$

where the heat flux has been related to the temperature via Fourier's law

$$q_{L/S} = -a_{L/S} \, \nabla T_{L/S}. \qquad (8)$$

The quantities a_L, a_S denote the liquid and solid thermal conductivities, respectively. In order to present the mean curvature and the outer normal at the interface I we use the coordinate system of Figure 3:

$$\kappa_M(x) = \frac{y''(x)}{2(1 + y'(x)^2)^{3/2}} \quad \text{and} \quad \vec{n}(x) = (-y(x), 1)\frac{1}{\sqrt{1 + y'(x)^2}}, \qquad (9)$$

thus we have

$$T_I(x) = \bar{T}(p_L) - \frac{\sigma T_m}{\lambda \bar{\rho}_S} \frac{y''(x)}{(1 + y'(x)^2)^{3/2}}. \qquad (10)$$

3.2 Boundary values

Finally we have to fix external boundary values for the problem (7). We assume that the temperature at the melt isotherm is given by $\bar{T}(p_L)$ and that we have a constant negative temperature gradient ∇T along the crucible wall, where the temperature reads in the coordinate system of Figure 3

$$h(x) = \bar{T}(p_L) - \frac{|\nabla T|}{\sin(\beta)}x. \qquad (11)$$

The solution of the general problem (7) will be addressed in a forthcoming paper. In the next section we briefly present the special case where the thermal conductivities of liquid and solid are equal.

3.3 Exact solution for equal thermal conductivities

For $a_L = a_S$ we obtain a solution of (7) by setting $T_L = h|_{\Omega_L}$ and $T_S = h|_{\Omega_S}$. In particular we get

$$T_I(x) = \bar{T}(p_L) - \frac{|\nabla T|}{\sin(\beta)}x. \qquad (12)$$

Comparing with (10), we end up with the following second order ordinary differential equation

$$\frac{y''(x)}{(1 + y'(x)^2)^{3/2}} = \frac{c}{\sin(\beta)}x, \qquad (13)$$

6

with the positive parameter $c = \dfrac{\bar{\rho}_S \lambda |\nabla T|}{\sigma T_m}$ and the boundary conditions

$$\begin{cases} \lim_{x \to 0} y'(x) & = & -\infty, & y'(L) & = & -\cot(\alpha - \beta), \\ \lim_{x \to 0} y(x) & = & \infty, & y(L) & = & L \cot(\beta) \end{cases} \tag{14}$$

The exact solution of (13) has been determined in appendix 6. It reads

$$y(x) = L(\alpha, \beta, c)\, \cot(\beta) + Y(x) - Y(L(\alpha, \beta, c)) \quad \text{for} \quad x \in (0, L], \tag{15}$$

with $L = \sqrt{\frac{2}{c} \sin(\beta)(1 - \cos(\alpha - \beta))}$. The function Y is given by

$$Y(x) = -\frac{1}{\tilde{c}} \left(\sqrt{4 - (\tilde{c}x)^2} - \ln \frac{x}{\sqrt{4 - (\tilde{c}x)^2} + 2} \right) \quad \text{with} \quad \tilde{c} = \sqrt{\frac{c}{\sin(\beta)}}. \tag{16}$$

Since the isotherms in the undercooled melt are parallel to the ordinate, for α greater than β the largest deviation from the melting temperature is at the triple point and can be calculated as

$$u_m(\alpha, \beta, c) = \bar{T}(p_L) - T_I(L(\alpha, \beta, c)) = \frac{|\nabla T|}{\sin(\beta)} L(\alpha, \beta, c) = |\nabla T| \sqrt{\frac{2}{c} \frac{(1 - \cos(\alpha - \beta))}{\sin(\beta)}} \tag{17}$$

One can easily prove that the undercooling u_m at $x = L(\alpha, \beta, c)$ is a monotonic increasing function of α and monotonic increasing function of β.

3.4 Crystal-melt interface with material data for gallium arsenide

In the numerical simulations we have used the following material data for GaAs:

$m = 1.2004 \times 10^{-25}$ kg (molecular mass)

$\nabla T = -500$ K m^{-1} (temperature gradient)

$T_m = 1511$ K (temperature at the congruent melting point) with the corresponding data

$\bar{p} = 2.77 \times 10^5 \; \frac{\text{N}}{\text{m}^2}, \; \bar{\rho}_L = 5.72 \times 10^3 \; \frac{\text{kg}}{\text{m}^3}, \; \bar{\rho}_S = 5.17 \times 10^3 \; \frac{\text{kg}}{\text{m}^3}, \; \sigma = 0.5 \; \frac{\text{N}}{\text{m}},$

$K_L = 7.55 \times 10^9 \; \frac{\text{N}}{\text{m}^2}, \; \lambda = 1.46 \times 10^6 \; \frac{\text{N m}}{\text{kg}}.$

Note that according to (5) $p_L < \bar{p}$ bar implies $\bar{T}(p_L) > T_m$ and for $p_L > \bar{p}$ bar we have $\bar{T}(p_L) < T_m$.

Figure 4 shows shape and location of the crystal-melt interface for different parameter values α, β and for $p_L = \bar{p}$. We observe that the deviation of the interface from
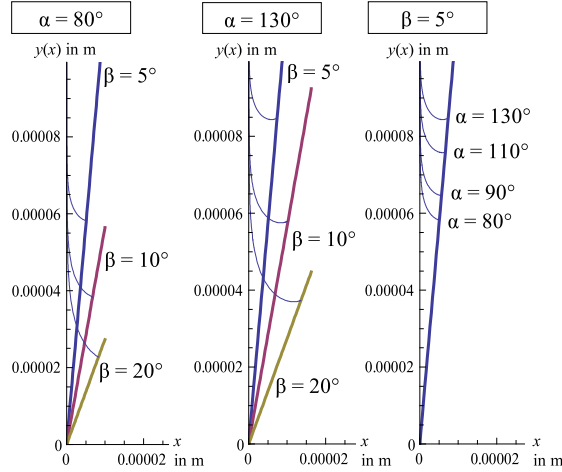
Figure 4: *Crystal-melt interface*

the melting isotherm increases for decreasing β and increasing α. Exploitation of (17) reveals the following: For equal thermal conductivities of liquid and solid and in the selected parameter range, the maximal undercooling is 0.137185, which is at least ten times less than the expected one, which is about 2 K for the application at hand. This is possible, but it requires $\beta < 0.002$.
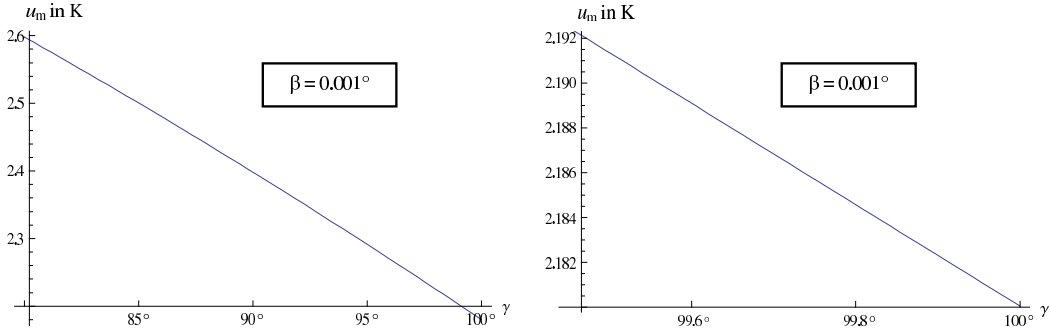

Figure 5: *Undercooling due to surface tension as a function of the contact angle γ for given melting isotherm angle β.*

4 Homogeneous and heterogeneous nucleation in the melt

4.1 Setting of the problem

In this chapter we study the possibility of the formation of a new solid nucleus in the undercooled region of the melt. We distinguish between homogeneous nucleation, due to random encounters of atoms in the liquid phase by undercooling or/and

supersaturation, and heterogeneous nucleation, which takes place at the wall of the vessel and depends on its material properties and on the geometry. We provide the wall with defects that may essentially assist heterogeneous nucleation. The defects are modelled here by four different cases as it is indicated by Figures 6 and 7. We denote by γ the contact angle at the triple point and by φ the apex cone angle as indicated in Figure 6.
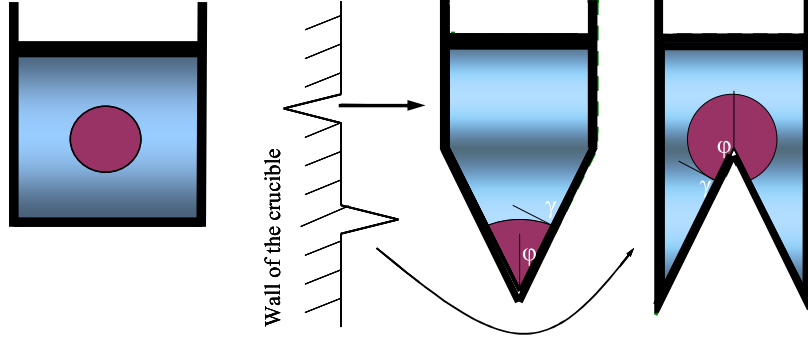

Figure 6: *Nucleation in the melt. Left: homogeneous. Middle and Right: heterogeneous.*

To simplify matters, we assume that the crystal is spherical. For the system in equilibrium we have the Gibbs-Thomson formula (6)

$$T_I = \bar{T}(p_L) - \frac{\sigma T_m}{\lambda \bar{\rho}_S} \frac{2}{r_{crit}}, \tag{18}$$

where r_{crit} denotes the so-called critical radius for nucleation. The interpretation is as follows: If due to random encounters a nucleus forms with less that n_{crit} atoms, which denotes the number of particles contained in a cluster with radius r_{crit}, then it will shrink till it vanishes, whereas cluster with $n > n_{crit}$ will grow further on. We assume, that a realistic number of atoms, that can accidentally collide in the liquid phase by fluctuation, is less than one hundred. Thus, only in a system, where n_{crit} is small enough, nucleation can take place.
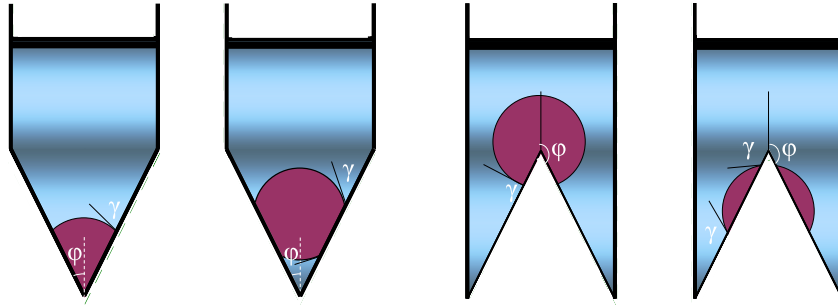

Figure 7: *Setting for different cone angles*

Re-arranging equation (18) we get

$$r_{crit} = \frac{2\sigma T_m}{\lambda \bar{\rho}_S} \frac{1}{u} \quad \text{with} \quad u = \bar{T}(p_L) - T_I. \tag{19}$$

9

For the four considered cases in Figure 7 we may relate the critical radius to the corresponding particle number n, by

$$V_S = \frac{m_S}{\rho_s} = \frac{m\,n}{\rho_s} \approx \frac{m\,n}{\bar{\rho}_s} \quad \text{and} \quad V_S = F(\gamma, \varphi)\,\frac{4\pi}{3} r^3. \tag{20}$$

Herein φ denotes the semi-cone angle, γ is the contact angle and m_S and m denote the mass of the solid cluster respectively the mass of an atom. Clearly we have $(20)_1$, whereas the proof of $(20)_2$ and the explicit form of the function F for the four cases considered in Figure 7 need some simple but quite tedious geometric calculations. They are listed in (21). In the case of homogeneous nucleation, where the nucleus has no contact to the wall, we have $F = 1$.

$$F(\gamma, \varphi) = \begin{cases} 1 & \begin{cases} \text{if } 0 \le \varphi \le 90° \text{ and } \gamma = 0° \\ \text{or } 90° \le \varphi < 180° \text{ and } \gamma \le \varphi - 90° \end{cases} \\[2em] 1 - \cos(\varphi)\sin^3(\gamma) & \text{if } 0 \le \varphi \le 90° \text{ and } 0° \le \gamma \le 90° - \varphi \\[2em] \frac{1-\sin(\gamma-\varphi)}{2} + \frac{\cos(\gamma)\cos^2(\gamma-\varphi)}{4\sin(\varphi)} & \begin{cases} \text{if } 0 \le \varphi \le 90° \\ \quad \text{and } 90° - \varphi \le \gamma \le 90° + \varphi \\ \text{or } 90° \le \varphi < 180° \\ \quad \text{and } \varphi - 90° \le \gamma \le 270° - \varphi \end{cases} \\[2em] -\cos(\varphi)\sin^3(\gamma) & \begin{array}{l} \text{if } 90° \le \varphi < 180° \\ \quad \text{and } 270° - \varphi \le \gamma \le 180° \end{array} \\[2em] 0 & \begin{cases} \text{if } 0° \le \varphi \le 90° \text{ and } 90° + \varphi \le \gamma \le 180° \\ \text{or } 90° \le \varphi < 180° \text{ and } \gamma = 180° \end{cases} \end{cases} \tag{21}$$

Thus the critical particle number is controlled by the undercooling and the geometric function F that takes care for the considered wall defect.

$$n_{crit} = F(\gamma, \varphi)\,\frac{4\pi}{3}\frac{\bar{\rho}_S}{m} r_{crit}^3 = F(\gamma, \varphi)\,\frac{4\pi}{3}\frac{\bar{\rho}_S}{m}\left(\frac{2\sigma T_m}{\lambda \bar{\rho}_S}\frac{1}{u}\right)^3. \tag{22}$$

Note that the critical radius is the same for both homogeneous and heterogeneous nucleation, whereas the corresponding particle number may strongly differ depending on the different volumes of the critical cluster.

The circumstances for homogenous nucleation, i.e. $F = 1$, are illustrated in Figure 8, which represents how the particle number of a critical cluster depends on the undercooling. For three selected particle numbers we may read rom Table 4.1 the corresponding values of undercooling.

A comparison with the material data given in Section 3.4 reveals that homogenous nucleation first sets in if the undercooling is 240 K. However, according to [EKSJ] nucleation occurs at the container wall near to the triple point already for an undercooling of a few Kelvin. We conclude that this can only be understood if the
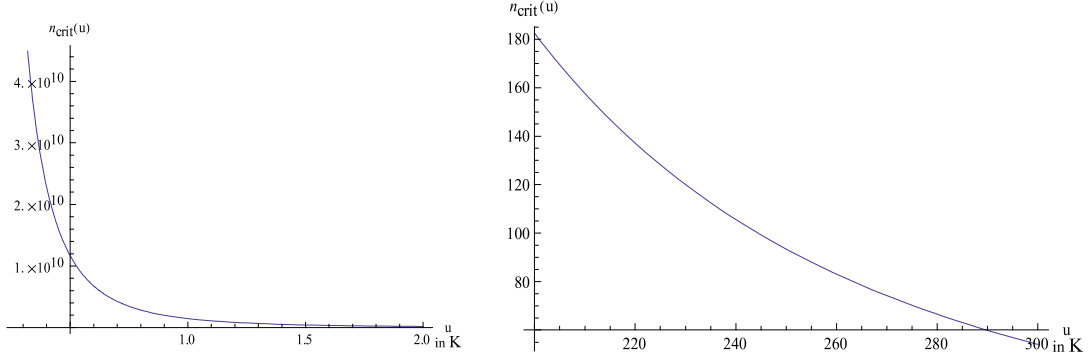
10

Figure 8: *Dependence of the critical particle number on the undercooling in the homogeneous case*

Table 1:

u in K	0.137	3	240
n_{crit}	5.6 10^{11}	53 673 030	105

observed phenomenon is due to heterogeneous nucleation, requiring

$$0 < F \ll 1. \tag{23}$$

For an illustration we refer to Table 2 where n_{crit} values for different parameter constellations are given, and Figure 9 shows for different cone angles the behavior of F as a function of the contact angle. We observe that we must have $\gamma > 90°$
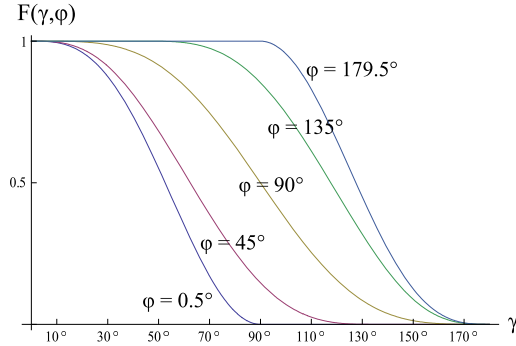

Figure 9: *F for different cone angles*

in order to satisfy the condition (23). We read off from Table 2 that heterogenous nucleation already sets in at a wall defect that represents a disruption with cone angle $\varphi < 11°$ and if the contact angle is $\gamma = 100°$, see the first case of Figure 7.

5   Conclusions

The two main results from Sections 3 and 4 may be summarized as follows: At first we calculate for given isotherm angle β and given contact angle γ the undercooling.

11

Table 2:

$u = 3$ K	r in 10^{-8} m	$n_{\text{crit}}^{\text{hom}}$	$n_{\text{crit}}^{\text{het}}$
$F = 0.1$ $(\gamma = 80°,\ \varphi = 20°)$ $(\gamma = 90°,\ \varphi = 37°)$ $(\gamma = 100°,\ \varphi = 51°)$	6.676775	53 673 030	5 367 303
$F = 0.01$ $(\gamma = 90°,\ \varphi = 12°)$ $(\gamma = 100°,\ \varphi = 25°)$	6.676775	53 673 030	536 730
$F = 0.001$ $(\gamma = 90°,\ \varphi = 3.7°)$ $(\gamma = 100°,\ \varphi = 16°)$	6.676775	53 673 030	53 673
$F = 0.0001$ $(\gamma = 90°,\ \varphi = 1.1°)$ $(\gamma = 100°,\ \varphi = 12.6°)$	6.676775	53 673 030	5 367
$F = 0.00001$ $(\gamma = 100°,\ \varphi = 11.14°)$	6.676775	53 673 030	537
$F = 0.000001$ $(\gamma = 100°,\ \varphi = 10.52°)$	6.676775	53 673 030	54

Moreover we assume that the defect of the crucible wall in the vicinity of the triple point is a disruption with cone angle φ. By means of equations (22) and (17) we then calculate the number of atoms in a nucleus of critical size, see Figures 10 and 11. Thus again a contact angle $\gamma > 90°$ is needed for the formation of a nucleus.
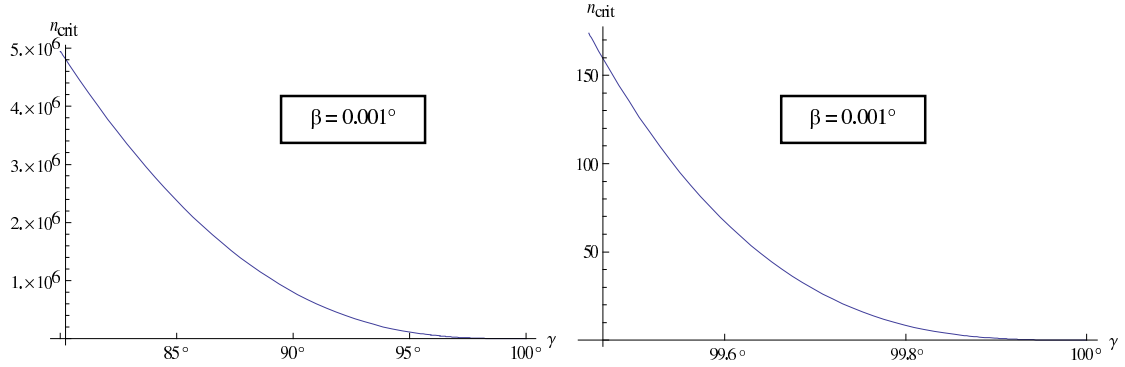

Figure 10: *The critical particle number as a function of the contact angle γ for heterogenous nucleation at a wall defect, represented by φ. According to Figure 3.4, which gives the corresponding undercooling, the melting isotherm angle β is 0.001.*
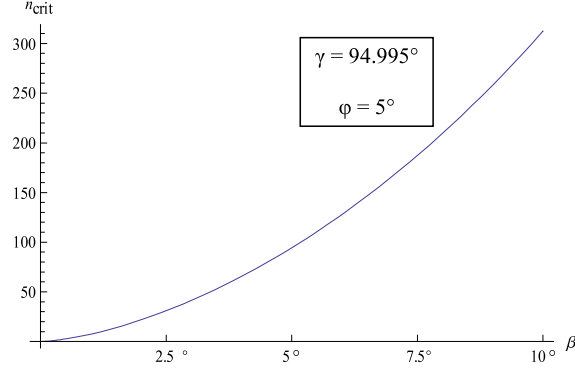
12

Figure 11: *Dependence of the critical particle number on the melting isotherm angle β for given values of cone angle φ and contact angle γ.*

6 Appendix

Our aim in this section is to identify the function $y(x)$ describing the interface between the crystal and the undercooled melt. To this end, we consider the second order ordinary differential equation

$$\frac{y''(x)}{(1 + y'(x)^2)^{3/2}} = \frac{c}{\sin(\beta)}x \quad \text{in} \quad [0, L], \tag{24}$$

where c is a positive parameter and L still to be determined by means of the given boundary values for y

$$\begin{cases} \lim_{x \to 0} y'(x) = -\infty, & y'(L) = -\cot(\alpha - \beta), \\ \lim_{x \to 0} y(x) = \infty, & y(L) = L \cot(\beta). \end{cases} \tag{25}$$

We solve the equation (24) in five steps:

1. We integrate (24) over the interval $[0, x]$ and use the initial value $\lim_{x \to 0} y'(x) = -\infty$ to get the algebraic equation in the new variable $u = y'$

$$\frac{u(x)}{(1 + u(x)^2)^{1/2}} = a(x) - 1 \quad \text{in} \quad [0, \infty), \tag{26}$$

with $a(x) = \frac{c}{2\sin(\beta)}x^2$.

2. We calculate from (26) for $x = L$ that

$$L = \sqrt{\frac{2}{c}\sin(\beta)(1 - \cos(\alpha - \beta))}. \tag{27}$$

3. We solve the equation (26) in $u(x)$, keeping in mind that u and $a - 1$ have the same sign, to obtain

$$u(x) = \frac{a(x) - 1}{\sqrt{a(x)(2 - a(x))}} \quad \text{for} \quad x \in \left(0, 2\sqrt{\frac{\sin(\beta)}{c}}\right), \tag{28}$$

13

which corresponds to the condition that the expression $a(x)(2 - a(x))$ should be strict positive. Note that the interval $[0, L]$ is always included in the domain of the solution above.

4. We integrate (28) over $[x, L]$ with the boundary value $y(L) = L \cot(\beta)$ to get the solution (15).

References

[DK]   W. Dreyer and C. Kraus, *The equilibria of vapour-liquid systems revisited*, WIAS preprint no. 1238, 2007.

[EKSJ] S. Eichler, U. Krezer, M. Scheffer-Czygan and M. Jurisch, *Polykristallines Wachstum beim VGF-Verfahren - Gibbs-Thompson-Effekt am Tripelpunkt?*, Talk for the III-V-Arbeitskreis der DGKK, Freiberger Compound Materials, April 2005.

[Hur]   *A mechanism for twin formation during Czochralski and encapsulated vertical Bridgman growth of III-V compound semiconductors*, Journal of Crystal Growth 147 (1995) p. 239–250.